

Hydraulic jumps at drop and abrupt enlargement in rectangular channel

Les ressauts hydrauliques liés aux dénivellations et aux élargissements brusques en canal rectangulaire

GIOVANNI B. FERRERI, *Researcher, Temporary Professor of 'Hydraulics', Dept. of Hydraulic Engineering and Environmental Applications, University of Palermo, Viale delle Scienze, 90128 Palermo, Italy*

CARMELO NASELLO, *Researcher, Temporary Professor of 'Hydraulic Infrastructure Works', Dept. of Hydraulic Engineering and Environmental Applications, University of Palermo, Viale delle Scienze, 90128 Palermo, Italy*

ABSTRACT

The different types of hydraulic jumps that occur in a rectangular channel at an abrupt increase in section are experimentally studied. The abrupt section increase is due to both a drop and an increase in the channel width. Experiments were carried out with three different values of the ratio L/l between the channel widths respectively downstream and upstream of the abrupt section increase. For each L/l value five values of Froude number F_1 of the supercritical flow upstream of the section increase were considered, and for each of them five values of the depth y_1 of the same flow. The experiments showed that, as the depth y_2 of the downstream subcritical flow increases, several types of hydraulic jumps occur. The sequence of hydraulic jump types and several characteristics of hydraulic jumps of the same type change with the flow parameters L/l , F_1 and s/y_1 , with s the drop height. Physical explanations of these changes are proposed, based on both direct observation of phenomena and comparison with results of other authors relative to the cases of either drop only or enlargement only.

RÉSUMÉ

On étudie expérimentalement les différents types de ressauts hydrauliques liés à une augmentation brusque de section en canal rectangulaire. L'augmentation brusque de section est due ici à la fois à une dénivellation et à un élargissement du canal. Les expériences ont été faites pour trois valeurs du rapport L/l entre les largeurs respectives du canal, à l'aval et à l'amont du changement de section. Pour chaque valeur de L/l , on a considéré cinq valeurs du nombre de Froude F_1 de l'écoulement torrentiel à l'amont de l'élargissement, et pour chacune d'elles, cinq valeurs de la profondeur y_1 du même écoulement. Les expériences ont montré que lorsque la profondeur y_2 de l'écoulement fluvial à l'aval augmente, il se produit plusieurs types de ressauts hydrauliques. La succession des différents types, et plusieurs caractéristiques des ressauts de même type, varient avec les paramètres L/l , F_1 , et s/y_1 de l'écoulement, s étant la hauteur de dénivellation. Des explications physiques de ces variations sont proposées; elles sont basées sur l'observation directe des phénomènes, ainsi que sur la comparaison avec des résultats obtenus par différents auteurs dans des cas présentant soit une dénivellation, soit un élargissement.

1 Introduction

Many hydraulic works (i.e. urban drainage networks, river channelizations, spillways, irrigation channels) require a flow transition from supercritical to subcritical, the relative hydraulic jump being steadily located within a certain short channel stretch (stilling basin). Usually, at the extreme sections of the channel stretch the momentum of the supercritical flow (upstream controlled) differs from that of the subcritical flow (downstream controlled): without suitable measures, the hydraulic jump would be located outside the stretch itself.

If the momentum of the supercritical flow exceeds that of the subcritical one, the steady location of the hydraulic jump within the stilling basin is obtained by means of a bottom rise [8, 13] or a reduction in the channel width [15] at the end of the stilling basin, i.e. the section of the downstream channel is reduced. By contrast, if the momentum of the subcritical flow exceeds that of the supercritical one, the jump within the stilling basin is obtained by means of a drop [8, 13] or an enlargement of the channel width [6], i.e. the section of the downstream channel is increased. In many situations, each of the above measures (either bottom rise or width reduction, either drop or enlargement) can by itself prove able to steadily locate the jump within the stilling basin. However, specific hydraulic and building situations could require a combi-

nation of bottom rise and width reduction or drop and enlargement. Single measures have been widely studied by many authors, whose experimental results allow a satisfactory design of the works. Bottom rise added to narrowing, very frequent in stilling basins downstream of barrages, has also been widely studied. By contrast, it is not easy to find studies concerning section increase by a drop combined with an enlargement, even though it is frequently adopted too in practice.

For this reason, an experimental research was started in the Department of Hydraulic Engineering and Environmental Applications of the University of Palermo (Italy), with the aim of studying the latter measure in a rectangular channel. Gangitano [5] stated that, when a drop is combined with an enlargement, the typical hydraulic phenomena of each measure overlap, reciprocally influencing each other, and produce hydraulic jumps whose overall characteristics at times are mainly referable to those of drop only, at other times to those of enlargement only, while yet other times the jumps just have autonomous characteristics. Therefore, to classify the jump types observed when both the measures are adopted, in the present paper first the main results of other authors relative to drop only and enlargement only are briefly reported, and then the results of the present research are expounded.

Revision received June 27, 2001. Open for discussion till December 31, 2002.

2 Previous studies about drop only or enlargement only

Most of the papers found in the literature relating to abrupt section increase concern drop only, which is mainly studied in the particular case of a rectangular channel section (bidimensional flow). A smaller number of papers concern abrupt enlargement only. All the papers study the link between the conjugate depths of the different types of jumps and describe the phenomena that characterize them; several papers also study the velocity distribution in sections or the bottom stress distribution or the positions of jumps.

Relatively to *drop only*, for a fixed depth y_1 of the flow upstream of the drop, whose mean velocity is V_1 , and hence its Froude number is

$$F_1 = V_1 / \sqrt{gy_1} \quad (1)$$

through papers by several authors [7, 8, 12, 13, 19, 20, 21] we evince that, as the depth y_2 of the subcritical flow downstream of the drop increases, five types of jumps occur. The first jump considered, for the smallest y_2 values, is the so-called *B-min jump* (Fig. 1a), located immediately downstream of the impact point of the nappe with the bottom of the downstream channel. With an increase in y_2 the *B jump* occurs (Fig. 1b), further back than the previous one, which submerges the final part of the nappe. With yet another increase in y_2 the *undulated jump* occurs (Fig. 1c), in which there is not the roller typical of hydraulic jumps but a wave train appears that is propagated downstream. From the building viewpoint, it must be pointed out that generally such wave train cannot be contained within works with an acceptable length. When the undulated jump appears, the nappe is still bent down, but then it bends upwards as y_2 increases. Because of a further increase of y_2 , the nappe rears, producing the *Wave jump* (Fig. 1d), whose main characteristics are a high steady wave and two eddies respectively located below and downstream of the nappe. The height of the steady wave, from the bottom, exceeds even 50% the depth y_2 [12], and hence calls for very high side containment walls. If y_2 increases still further, the steady wave disappears and the *A jump* occurs (Fig. 1e), whose characteristic is the 'classic' roller of the hydraulic jump in a prismatic channel, but

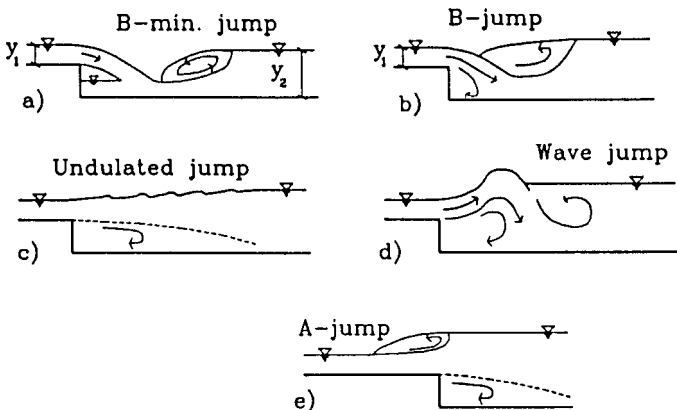


Fig. 1. Types of jumps at drop only that occur as depth y_2 increases.

is located astraddle the drop section.

In the case of *enlargement only* of the channel, whose width increases from l to L , through papers by several researchers [1, 6, 11, 17, 18, 22] we evince that a sequence of jumps occurs too as y_2 increases, for fixed upstream hydraulic conditions F_1 and y_1 . Fig. 2 shows the planimetric shape of the jump front (i.e. the upstream border of the jump roller) as it moves upstream because of the increase in y_2 . When there is not a subcritical flow downstream of the enlargement, the supercritical flow swiftly enlarges until it reaches the channel side walls in section B-B. Here, because of reflection on the walls, two steady waves occur, whose fronts converge on the channel axis in section D-D. Two other steady waves from this point originate, this time diverging. The phenomenon downstream recurs with characteristics analogous to those as far as section D-D.

The first hydraulic jump observed [17], for the smallest y_2 values, has a mixtilinear front (Fig. 2a). When the front is located in section D-D, it consists of two symmetric V. With an increase in y_2 , the front moves upstream of section D-D: on the outside of the steady waves the two V's persist, while between them the front is nearly straight. With a further increase in y_2 the front 'straightens' until the *Repelled jump (R-jump)* occurs [1, 17, 22]. The latter constitutes the limit situation in which there is a clearly localised jump front, because a further slight increase in y_2 causes sudden and radical changes in the overall flow. Indeed, near one of the two walls the subcritical flow 'breaks' the front of the repelled jump, moves upstream and deflects the supercritical flow toward the opposite wall (Fig. 2b). Therefore the flow proves to be asymmetric. The front break can indifferently occur on either wall, depending on accidental and instantaneous disturbances due to highly developed turbulence. Because of the asymmetry and the strong tridimensionality of the flow the phenomenon is called *Spatial jump (S-jump)* by Bremen and Hager [1]. Noseda [18] and Rajaratnam and Subramanya [22] report a particular periodic

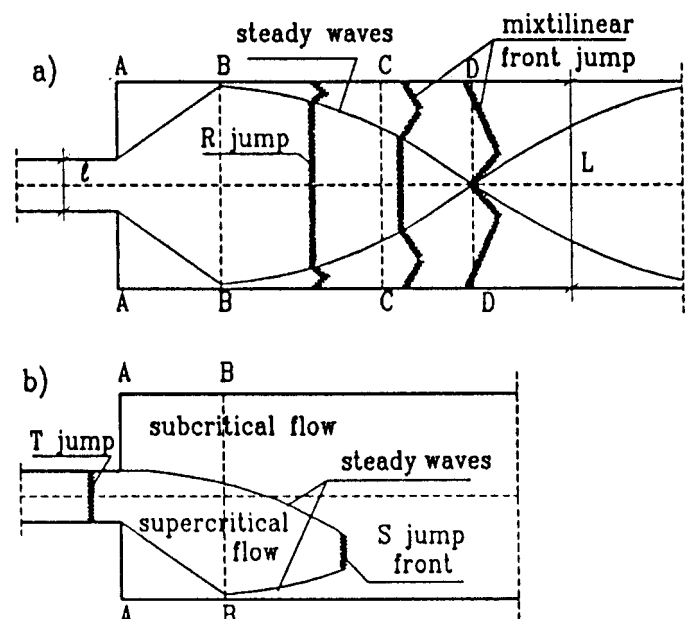


Fig. 2. Planimetric shape and location of jump front at enlargement only as depth y_2 increases.

behaviour: the supercritical flow alternatively goes towards either wall. According to Nosedá the oscillation occurs when $L/l > 6$, while for $L/l < 6$ the supercritical flow steadily keeps the asymmetric disposition that was established when the front broke.

With a further increase in y_2 , the subcritical flow submerges the supercritical one more and more, the aforesaid periodic phenomena disappear and a new hydraulic jump occurs, located astraddle the enlargement section [1]. This jump is called *Transition jump (T-jump)* because it precedes the ‘classic’ hydraulic jump, wholly contained within the upstream channel which is l wide. When the T-jump occurs the flow is still sensibly asymmetric. If y_2 increases, the jump even further moves upstream, while its front gradually places itself orthogonally to the channel axis.

3 Experimental equipment and experiment modalities

Experiments with drop and enlargement were carried out by us in a rectangular flume with level bottom, expressly built in the laboratory of the Department. The experiments were organised in three series, with ‘enlargement ratios’ $L/l = 4/3, 4/2$ and $4/1$, so that it was possible to observe how, as L/l increases, the characteristics of the different jump types change as the tridimensional characteristics of flow grow.

The experimental equipment is shown in Fig. 3. Water arrives with a discharge Q in a tank in which several pierced walls are located to still the flow before it enters the flume. The latter begins inside the tank, so that the flow approaches the gate with the streamlines sensibly straight and parallel. The flume is made in Plexiglas, has width $L=40$ cm and consists of two level reaches, respectively 0.80 and 5.70 m long, separated by a drop of height $s=10$ cm. In the three experiment series, the downstream reach maintains the width $L=40$ cm, while the upstream one has a width of $l=30, 20$ and 10 cm. The width l is obtained by inserting in the flume two vertical walls in Plexiglas equidistant from its axis. A sharp gate, in the reach wide l , makes it possible to control the supercritical flow upstream of the drop. The depth y_1 is measured by a water-gauge with decimal nonius. Because of surface ripples the depth y_1 was assumed equal to the mean of the measures in five verticals in the section located 40 cm upstream of the drop. The depth y_2 of the subcritical flow downstream of the drop is measured in the flume axis by a piezometer tapped on the bottom.

Four other piezometers, very close to one another and placed on the vertical, detect pressure distribution in the centre of the drop wall. Finally, two piezometers tapped on the bottom measure the pressure heads y_a at the corners of the drop wall and the downstream flume walls. At the end of the flume there is a grid with a variable slope to control the depth y_2 .

For each of the three experimental series twenty-five experiments were carried out, with height of the gate sluice and Froude number F_1 of the supercritical flow as shown in Tab. 1. Each experiment was carried out as follows. First the end grid was laid flat, so that the flow everywhere was supercritical. Then, for the fixed height of the gate sluice, the discharge Q was varied and the relative depth y_1 was measured until the chosen F_1 value was obtained. Slightly tilting the grid, in the final reach the flow turned into subcritical with depth y_2 . The grid slope was then increased step by step, causing the hydraulic jump to move upstream. The experiment finished when the jump front was localised in the l wide reach upstream of the drop, slightly downstream of the gate.

4 Types of hydraulic jumps observed

As stated in the introduction, when drop and enlargement are combined the types of hydraulic jumps that occur are the effect of overlapping and reciprocal influence of the hydraulic phenomena typical of each of the two measures. For fixed system sizes, i. e. l, L and s , to describe the examined flow, in which the friction forces are negligible with respect to the pressure forces, the force of gravity and the forces of inertia, two further lengths are necessary and sufficient, which also characterise it from the hydraulic viewpoint. We chose the critical depth k_1 of the flow in the upstream channel, that takes the discharge Q into account, and the depth y_1 that determines the velocity of the flow approaching the drop. The five lengths make it possible to form the following four dimensionless parameters ‘typical’ of the overall flow: the ‘enlargement ratio’ L/l , the relative drop height s/y_1 , the ‘aspect ratio’ of the upstream section y_1/l , on which the characteristics of the nappe depend [3], and obviously the Froude number (Eq. 1), which can also be written:

$$F_1 = \left(\frac{k_1}{y_1} \right)^{3/2} = \frac{Q}{g^{1/2} l y_1^{3/2}} \quad (2)$$

Tab. 1 Experimental values of F_1 for each height of the gate sluice.

Sluice gate height (cm)	F_1				
	2	3	4	5	6
1.5	2	3	4	5	6
2.0	-	-	4	5	6
2.5	2	3	4	5	6
3.0	-	-	-	5	6
4.0	2	3	4	5	6
6.0	2	3	4	-	-
9.0	2	3	-	-	-

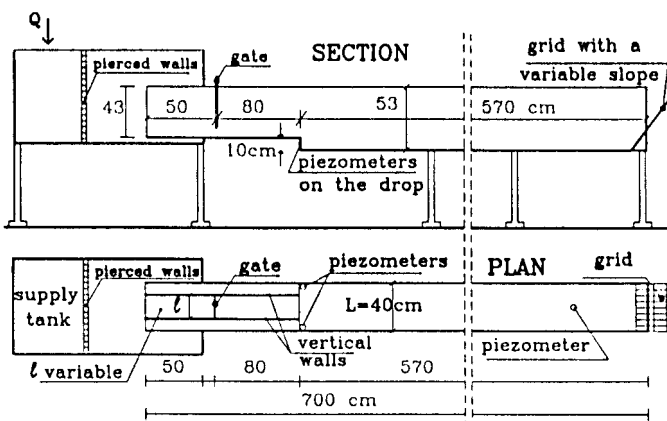


Fig. 3. Experimental equipment.

which, as is known, expresses the importance of the forces of inertia with respect to the force of gravity.

It is easy to forecast that, for given s/y_1 , F_1 and y_1/l , as the enlargement ratio L/l increases the tridimensional characteristics of flow due to the enlargement will grow. By contrast, for given s/y_1 , L/l and y_1/l , as F_1 increases the aforesaid characteristics weaken, because of the increase in momentum both of the nappe and of the supercritical flow downstream of the drop; it is therefore more difficult for the latter to be circled by the downstream subcritical flow. By contrast, one cannot immediately forecast the effect either of an increase in the aspect ratio y_1/l for given s/y_1 , F_1 and L/l , or of an increase in the relative depth of the drop s/y_1 for given F_1 , L/l and y_1/l . In fact, an increase in y_1/l , if due to an increase in y_1 , also involves an increase in s , while if it is due to a decrease in l it also involves a decrease in L . Analogous considerations are valid for an increase in s/y_1 , for given other parameters, due to a decrease in y_1 or an increase in s . It must be pointed out that an increase in s/y_1 for a given F_1 causes an increase in the angle α of incidence of the nappe with the downstream channel bottom (Fig. 4). It is easy to recognize [24] that, as α increases, the discharge Q_I making for downstream decreases with respect to the discharge Q_{II} that makes for the drop. Of course, this has consequences for the relative momentum M_1 and the characteristics of the hydraulic jump downstream.

Because of the evident complexity of the overall flow, the classification of the different hydraulic jumps observed by us, according to the *types* described below, was made on the basis of their *main* characteristics; hence, for given experimental s and L values, hydraulic jumps of the *same* type really present different particular phenomena depending on the values of the remaining parameters F_1 , y_1 and L/l . Indeed, for fixed values of s , L , F_1 and L/l , *two sequences* of hydraulic jumps were recognised as the depth y_2 increased: one for the smallest y_1 values, the other for the largest ones; the discriminant value y_1^* depends on the aforesaid parameters.

When the end grid is horizontal the stream is everywhere supercritical (Fig. 5a). The nappe, whose contour fully touches air, reaches the bottom of the downstream channel at a distance from section A-A that, for a given depth y_1 , obviously increases with the Froude number F_1 . After the impact with the bottom, particles diverge in all directions: most of them keep a velocity component toward downstream ('main' flow), while the remaining ones gain velocity component toward upstream. The latter reach section A-A, where they go some way up the drop wall, making a pool characterised by a very sprightly whirling motion.

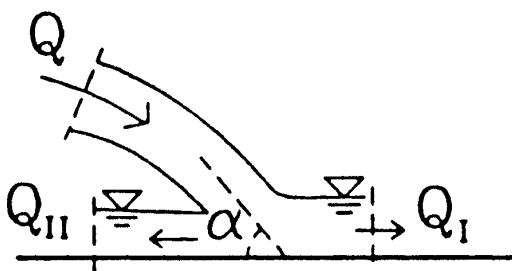


Fig. 4. Splitting of nappe on downstream channel bottom.

The pool has depths rapidly decreasing from the axis to the walls, along which, both on the right and the left of the main flow, two 'secondary' flows directed downstream occur. With the main flow the latter form the discharge Q . The main flow continuing downstream swiftly enlarges until it occupies the whole width L of the channel in section B-B. Here, the outermost particles crash into the channel walls and go some way up them. The latter then reflect the particles toward the axis. The reflected particles, for their part, crash into those of the innermost streamlines of the enlarging supercritical flow, leading to the formation of two steady waves, which extend downstream converging on the channel axis in section D-D. Two other steady waves, this time divergent, originate from the convergence point. The flow pattern just described qualitatively repeats itself downstream, giving the free surface a lozenge appearance. At the wave fronts the free surface is very steep. The water depths outside the waves are larger than the inside ones (see section C-C). The phenomena just described are analogous to those found in enlargement only and generally when a perturbation is produced in a supercritical flow, e.g. a bend [10] or an insertion of several piers [16].

In reality, the enlarging supercritical flow is not always able to occupy the whole width L of the channel in section B-B, but, for given s , L , F_1 and L/l , when $y_1 < y_1^*$, the reflection points in section B-B are *detached* from the channel walls (Fig. 5b). The space between the steady wave fronts and the walls is then occupied by two secondary flows that originate from the pool upstream of the nappe. Suitable measures made it possible to recognise that these secondary flows are subcritical (i.e. the main velocity along a vertical is smaller than the celerity \sqrt{gy} computed in the same vertical), and only after a more downstream section K-K do become supercritical.

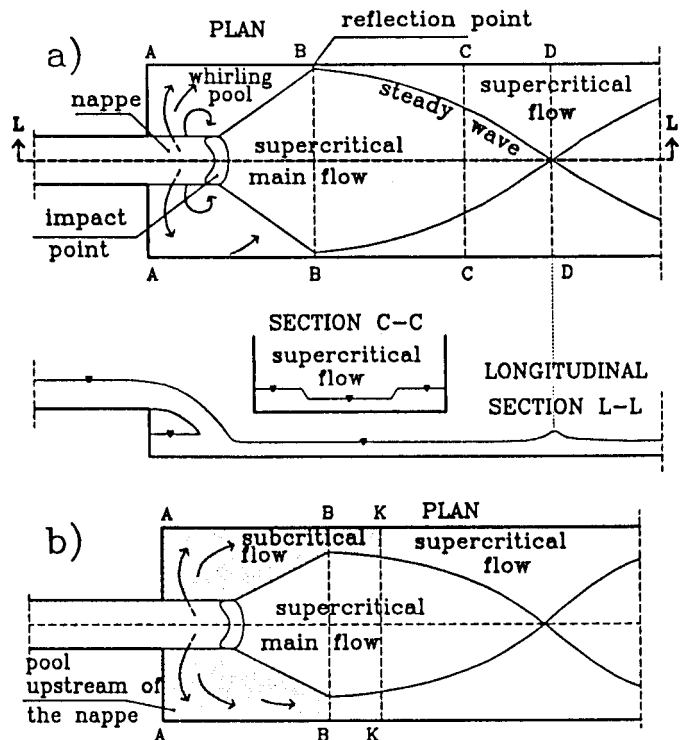


Fig. 5. Supercritical flow with horizontal grid: a) attached reflection points; b) detached reflection points.

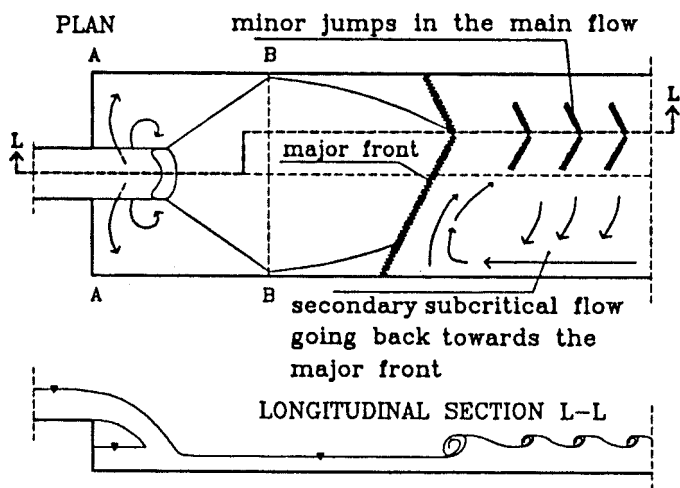


Fig. 6. Flow pattern of V-jump.

In short, the circumstance that $y_1 < y_1^*$ or $y_1 > y_1^*$ modifies not only the hydraulic jump sequence as the depth y_2 increases, but also the characteristics of the supercritical flow in the downstream channel.

Beginning to slightly tilt the grid, so that a subcritical flow occurs at the final stretch of the channel, the first hydraulic jump observed is the *V-jump*. Its front (Fig. 6) designs an asymmetric V with the vertex located upstream of section D-D, on one of the two steady waves of the supercritical flow. Downstream of the V front, numerous minor jumps occur, also with fronts V-shaped, whose vertexes are aligned with that of the major jump. These minor jumps involve only a part of the width L of the channel. In the remaining part, a secondary subcritical flow goes back toward the front of the major jump. Because of the presence of the aforesaid minor jumps the flow entrains a considerable quantity of air that is dragged as far as the channel end. Localisation of the main flow and of the jump vertexes on one side of the channel, and of the secondary flow on the opposite one, occurs in a quite casual way, depending on momentary instability factors that occur when the V-jump forms. However, after the flow takes on a certain asymmetric set-up, it steadily keeps it.

With an increase in y_2 the V-jump moves upstream. The V vertex follows the front of the steady wave approaching the channel wall, while the two sides of the V tend to line up themselves orthogonally to the channel axis. When a certain y_2 value is reached, the hydraulic jump changes appearance and characteristics: the next jump depends on whether that $y_1 > y_1^*$ (first sequence) or $y_1 < y_1^*$ (second sequence), i. e. on whether the reflection points in section B-B are respectively *attached to* or *detached from* the channel walls.

If $y_1 > y_1^*$ (reflection in attached points), the *Mixtilinear jump* (*ML-jump*) occurs (Fig. 7), analogous to that of enlargement only. The front, in the central stretch between the two steady waves, is almost rectilinear and perpendicular to the channel axis; between the waves and the walls, instead, it forms two V's.

A further increase in y_2 obviously causes the jump to draw back some more. When it is located a little downstream of section B-B (Fig. 8) it takes characteristics analogous to those of the repelled jump (*R-jump*) of enlargement only: therefore we shall still call it with the same name. The front of the R-jump is almost rectilinear and perpendicular to the channel axis in the lateral zones too, where, however, two short parts are slightly downstream of the central part. The reason why the jump front in the lateral parts is not aligned with that in the central part, in accordance with Nosedá [17] for enlargement only, is attributable to the different momentum per unit width of the lateral supercritical flows with respect to the central flow. Indeed, these flows have different depths and discharges per unit width.

Because the R-jump is located immediately downstream of reflection section B-B, a slight increase in y_2 causes it to move upstream of this section. Analogously to the case of enlargement only [1, 17, 22], near one of the two channel walls the subcritical flow 'breaks' the front of the R-jump and goes upstream toward section A-A (Fig. 9), partially submerging the enlarging supercritical flow. When the subcritical flow reaches section A-A, it goes toward the opposite wall, passes below the nappe and returns downstream. Because of the marked tridimensional characteristics of the flow, we will indicate this phenomenon as *Spatial*

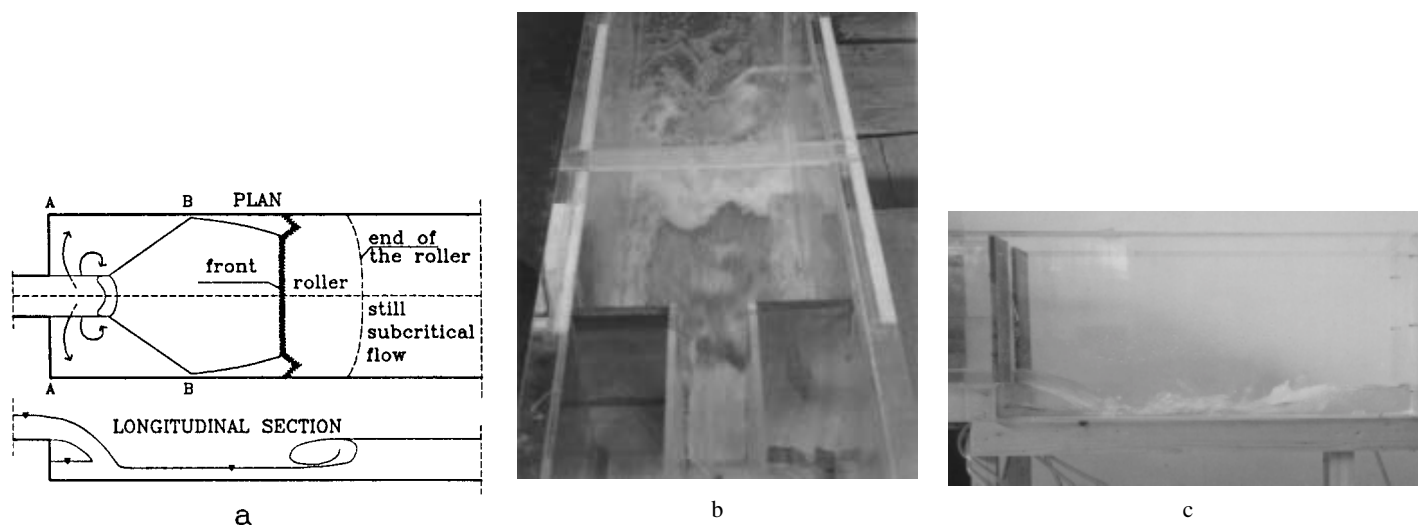


Fig. 7. Flow pattern of ML-jump: a) schematic depiction; b) top view; c) side view.

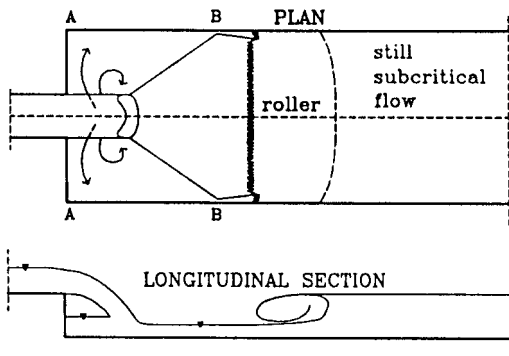


Fig. 8. Flow pattern of R-jump.

jump (*S-jump*), like the analogous jump of enlargement only. The enlarging supercritical flow is deflected toward the wall opposite to that near which the front break occurred. It takes on the appearance of a 'spindle', whose longitudinal axis, when the spindle appears, is oblique to the channel one. Around the tip and along the contour of the spindle a roller with a V-shaped front occurs. Downstream of the spindle, a main flow is made out that goes downstream forming several minor jumps, with their fronts V-shaped too, which separate as many short reaches of supercritical flows as alternate reaches of subcritical flows. The vertexes of these consecutive V's set out along the virtual curve line FG. Some of the particles of the main flow, after contributing to the formation of the aforesaid minor jumps, turn toward the opposite side and go to supply the secondary flow returning to section A-A. The break of the front of R-jump, which originates the S-jump, can indifferently occur near either wall of the channel. After one of the two possible asymmetric sets-up is established, it remains steady.

As y_2 increases, the subcritical flow gradually submerges the supercritical one, and the spindle shortens, i. e. its downstream vertex F moves upstream, while its longitudinal axis tends to set

itself parallel to the channel one. However, even when the spindle becomes practically symmetric (Fig. 10) the overall phenomenon still remains strongly asymmetric, so that we shall continue to call it S-jump. In these conditions, the line FG does not gradually approach the wall any more but 'collides' with the wall. The consequent crash of the particles against the wall, in addition to the superelevation of the free surface connected with it, produces a state of the streamlines in many respects different from that of Fig. 9. Besides, analogously to what was observed by Nosedá [18] and by Rajaratnam and Subramanya [22] for enlargement only, for the largest values of L/l periodic oscillation of the line FG is observed. The latter, rotating around the point F, moves now toward the right now toward the left side of the channel. The streamlines around the spindle are consequently modified. The period τ measured is between 10 and 90 s.

Because of a further rise in the downstream level, the spindle is submerged until it disappears: then the curve line FG remains, established at the nappe toe; along the same curve the free surface is very rough and the air entrainment considerable. The periodic oscillation, if already present, persists.

The hydraulic jumps described until now (V, ML, R and S) are referable to those of enlargement only, the next ones that we are going to describe to those of drop only.

When y_2 increases the end part of the nappe is submerged too. The upstream flow, the minor jumps and the virtual line FG disappear. Downstream of the nappe a big roller then forms (Fig. 11), which enlarges until it occupies the whole width of the channel. Because of the analogies between this jump and the one observed for drop only (Fig. 1b), we shall still call this phenomenon *B-jump*. When B-jump appears, the nappe is still aired underneath, because the depth y_a of the pool at the drop toe is smaller than the drop height s . With a further increase in y_2 the pool finally touches the down surface of the nappe ($y_a = s$), which then is no longer aired. Once $y_a > s$, the drop wall proves to be completely submerged. Consequently an *aired* B-jump (Ba) for $y_a < s$ and a *non-aired* B-jump (Bna) for $y_a \geq s$ can be distinguished.

If y_2 increases further, the plunge point of the nappe draws back. At a certain point, downstream of the nappe, in the upper part of the flow a supercritical central current is observed, which moves

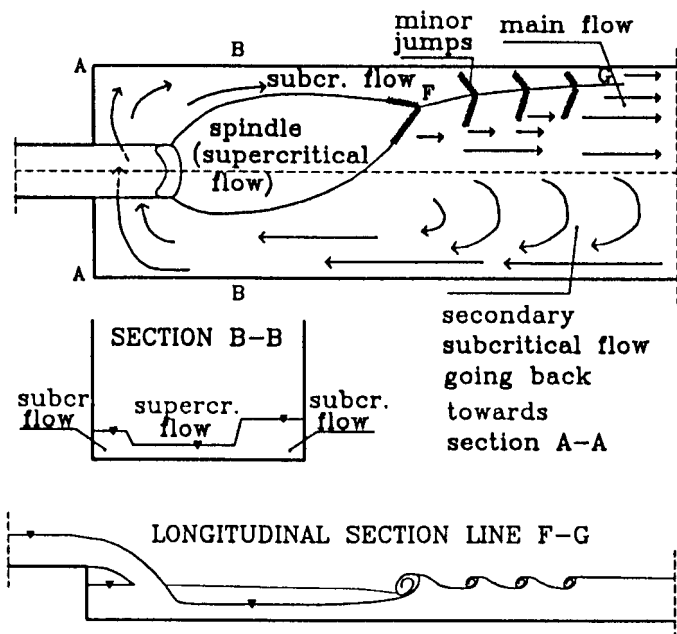


Fig. 9. Flow pattern of S-jump.

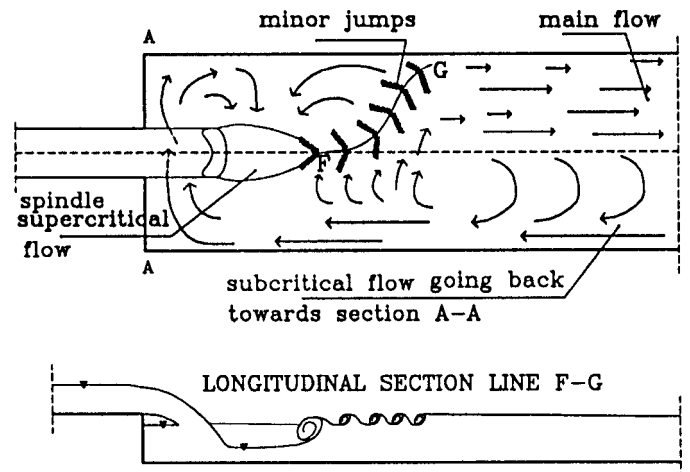


Fig. 10. Flow pattern of S-jump with symmetric spindle.

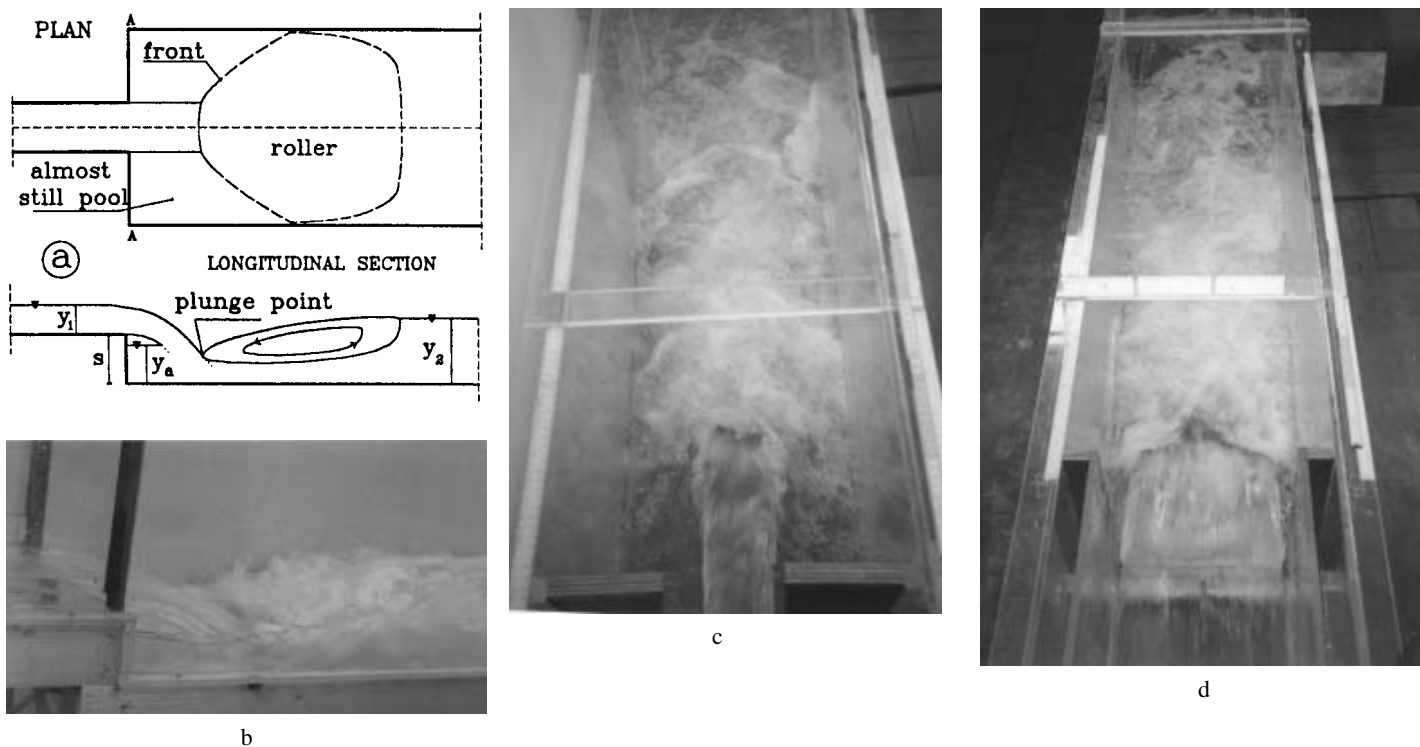


Fig. 11. Flow pattern of B-jump: a) schematic depiction; b) side view for $L/l = 4/3$; c) top view for $L/l = 4/1$; d) top view for $L/l = 4/3$.

between two subcritical wings (Fig. 12). On the free surface, the fronts of two steady waves intertwine, converging and diverging along the channel axis, and design several quadrilaterals. The quadrilateral vertexes situated on the channel axis are also the vertexes of V-shaped steady waves. The latter extend into the subcritical wings, and weaken downstream. We shall indicate this dissipative phenomenon as *Undulated jump (U-jump)*. As long as the mean piezometric head h_d along the axis of drop wall remains smaller than the elevation of the free surface in the upstream

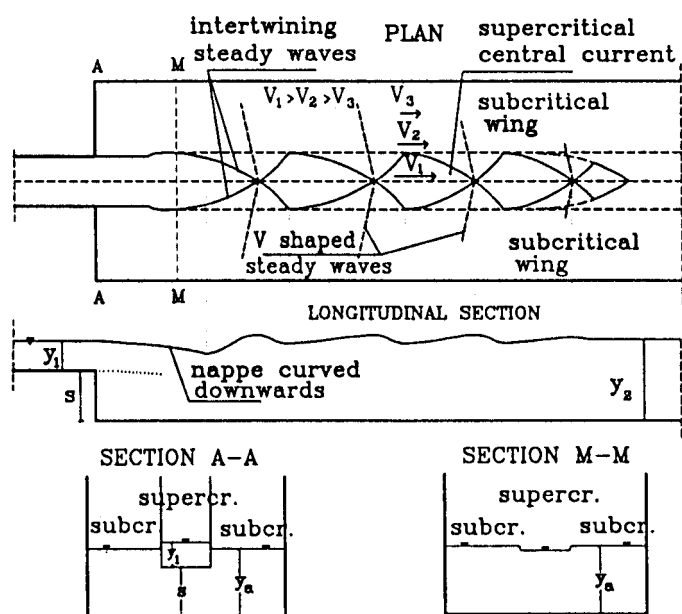


Fig. 12. Flow pattern of U-jump with nappe curved downwards.

channel, i. e. $h_d < s + y_1$ (Fig. 12), the nappe is curved downwards (*Ud-jump*), while for $h_d > s + y_1$ (Fig. 13) the nappe is curved upwards (*Uu-jump*). Because of the rise of the free surface between the central part and the lateral parts of section A-A, in the Uu-jump two steady waves are established at points P_1 and P_2 of the same section. The waves, absent in the Ud-jump, meet on the channel axis a little downstream. Indeed, for the largest experimental discharges the turbulence considerably strengthens, and a mixture of water and air forms in the central zone of the channel, so that the supercritical current and the subcritical wings can no longer be seen as clearly as shown in Figs. 12 and 13.

If y_2 increases, the quadrilateral design tends to disappear, the steady V fronts draw back upstream, as does the intersection point of the fronts established at P_1 and P_2 . At a certain point a surface roller appears, analogous to that of the 'classic' hydraulic jump in a prismatic channel, whose front is located upstream of section A-A (Fig. 14). This dissipative phenomenon corresponds to the A-jump of drop only [8, 13, 20]. However, we shall call it *Transition jump (T-jump)* because, with a further increase in y_2 , finally the *Classic jump (CL-jump)* occurs, entirely contained in the upstream channel wide l.

It must be pointed out that, because of the short length of the channel upstream of section A-A, the CL-jump only occurred for a few F_1 and y_1 values in our experiments.

In short, trying to simplify the interpretation of the phenomenon, which is indeed rich and complex, when $y_1 > y_1^*$ (first sequence), reflection in section B-B occurs at points attached to the walls and, with increases in y_2 , the jumps V, ML and R follow one another; then, after the break of the R-jump front, generally, unless what will be specified in the next section, the S-jump occurs, fol-

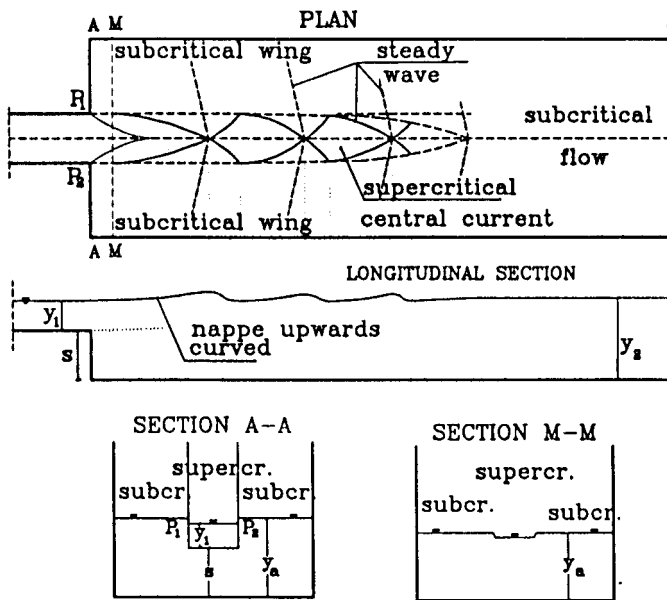


Fig. 13. Flow pattern of U-jump with nappe curved upwards.

lowed by Ba, Bna, U, T and CL jumps.

By contrast, when $y_1 < y_1^*$ (second sequence), reflection in section B-B occurs at points detached from the walls and there is already front break in V-jump. After the break, the S-jump *always* occurs, after which the sequence continues as the first one.

Detached reflection and front break in the V-jump instead of in the R-jump ($y_1 < y_1^*$) have a common main physical explanation. For fixed $s, L, L/l$ and F_1 , if y_1 decreases the velocity V_1 also decreases, and consequently the total momentum per unit width is reduced at each vertical of the same section of the supercritical flow in the downstream channel. The total momentum also decreases as a result of the increase in the relative depth s/y_1 of the drop that (see section 4, Fig. 4) causes a reduction, all other things being equal, in the discharge Q_1 of the supercritical main flow. All this, on one hand causes the enlarging supercritical flow not to succeed in reaching the walls, so that the reflection is detached. On the other hand, because the total momentum proves to be reduced, in particular along the front of the V-jump, a small and instantaneous local unbalance is sufficient for the total momentum of the subcritical downstream flow to succeed in being prevalent. Therefore, it submerges the supercritical flow and

modifies the overall pattern of the phenomenon. Moreover, when the reflection is detached, downstream of section B-B, the two secondary lateral flows have velocities which are significantly lower than that of the main flow and, hence, they are more easily submergible as a result of an increase in the depth y_2 of the subcritical downstream flow.

5 Existence ranges of the different types of hydraulic jumps

5.1 First experiment series ($L/l = 4/3$)

In the first experiment series the width l of the channel upstream of the drop and enlargement section A-A is equal to 30 cm ($L/l = 4/3$). The experimental results are reported in Tab. 2. Each column of the table is relative to a couple of F_1 and y_1 values, and reports the sequence of jumps observed as y_2 increases (y_2 increases from column toe to top). The experiment discharge is reported at the column top. The depth y_2 is read on the scale along the left edge of the table; the drop height $s=10$ cm is underlined on the scale, in order to make it easy to recognise the situations in which the downstream free surface overcomes the upstream bottom or even the upstream free surface. In each column, for several values of the depth y_2 , the corresponding values of the Froude number F_2 of the downstream subcritical flow are reported, computed assuming a uniform distribution of velocity in the section. For example, in the first column, for $y_2=18$ cm we read $F_2=0.26$. Over the sequence it is indicated whether the reflection in section B-B is attached ($y_1 > y_1^*$) or detached ($y_1 < y_1^*$); a dotted line separates the two situations and indicates between which y_1 values the discriminant value y_1^* falls: e. g., for $F_1=2$, y_1^* falls between $y_1=1.83$ and $y_1=2.71$ cm.

Analysis of the table shows that the first hydraulic jump observed, for the smallest y_2 values, is always the V-jump. As was previously stated, when the reflection is attached, after the V-jump the ML and R-jumps follow; by contrast, when the reflection is detached, after the V-jump there is the S-jump. The y_1^* value decreases as F_1 increases: e. g., for $F_1=2$ it is $1.83 < y_1^* < 2.71$ cm; for $F_1=5$ it is $1.22 < y_1^* < 1.44$ cm; for $F_1=6$ y_1^* probably proves to be smaller than the smallest experimental value $y_1=1.19$ cm. This result suggested the physical explanation given at the end of section 4. Indeed, with an increase in F_1 , with the same y_1 the velocity V_1 and nappe total momentum also increase. Thus, increasing F_1 , even for y_1 values becoming smaller and smaller: 1) the reflection remains attached and 2) the supercritical flow succeeds in opposing the upstream movement of the subcritical flow along the whole width of the channel.

After the R-jump (attached reflection; $y_1 > y_1^*$), generally we do not find an S-jump but a Ba-jump; the S-jump follows the R-jump only for $F_1=4, 5$ and 6, and only for the smallest y_1 values, i. e. for the smallest discharges Q and velocities V_1 . In this series, in the S-jump there is not the periodic oscillation of the virtual line FG. After the S-jump the Ba-jump always occurs.

In all the columns, starting from the Ba-jump, the sequence continues as described in section 4 (Bna, Ud, Uu and T).

It must be pointed out that, only in this experiment series (L/l little larger than 1), for $F_1 \geq 3$ a phenomenon oscillating in the lon-

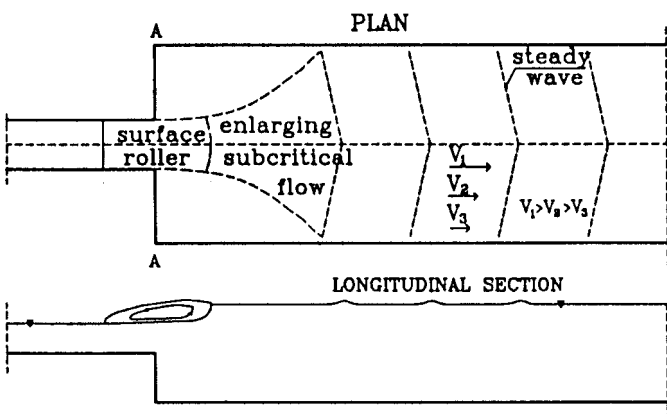
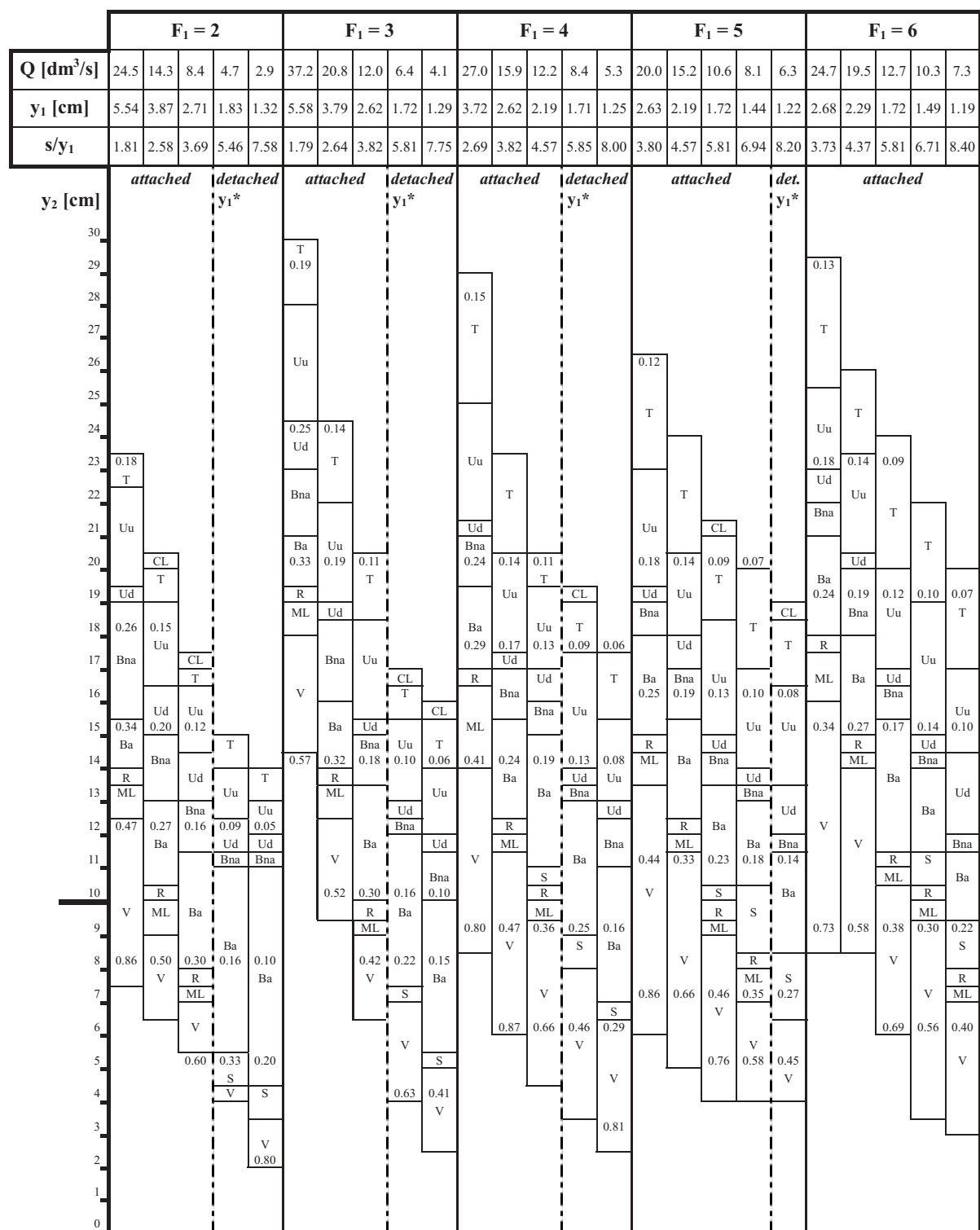


Fig. 14. Flow pattern of T-jump.

Tab. 2 Sequences of jumps for $L/l = 4/3$.



y_1^* = value of y_1 that marks attached and detached reflection
 0.81 = Froude number value in the subcritical downstream flow
 V = V-jump
 ML = Mixtilinear jump
 R = Repelled jump
 S = Spatial jump

Ba = B-jump aired
 Bna = B-jump non aired
 Ud = Undulated jump downwards curved
 Uu = Undulated jump upwards curved
 T = Transition jump
 CL = Classic jump

longitudinal direction occurs in the change from the Bna to the Ud-jump. This phenomenon, for given y_1 and F_1 , was observed within a narrow range of y_2 values. By contrast, outside this range each of the two jumps is *steady*. At time $t = 0$ the down-curved nappe of the Bna-jump plunges under the jump roller. Passing t ,

the nappe gradually weakens its curvature and moves more and more downstream its plunge point, until it almost wholly stretches and changes into a Ud-jump at time $t = \tau/2$. Then, in the range $\tau/2 < t < \tau$ the nappe again augments its down curvature and allows a wave to move upstream. Slightly downstream of the drop, the

Tab. 3 Sequences of jumps for $L/l = 4/2$.

	$F_1 = 2$					$F_1 = 3$					$F_1 = 4$					$F_1 = 5$					$F_1 = 6$									
Q [dm ³ /s]	15.5	9.5	5.0	2.8	2.0	24.2	14.0	7.4	3.8	2.8	33.2	19.2	9.7	5.1	3.5	23.9	13.6	7.1	6.1	4.4	16.0	12.9	8.6	6.8	5.3					
y_1 [cm]	5.35	3.87	2.52	1.69	1.37	5.50	3.82	2.50	1.60	1.31	5.60	3.88	2.47	1.60	1.25	3.88	2.66	1.72	1.56	1.26	2.63	2.28	1.73	1.49	1.25					
s/y_1	1.87	2.58	3.97	5.92	7.30	1.82	2.62	4.00	6.25	7.63	1.79	2.58	4.05	6.25	8.00	2.58	3.76	5.81	6.41	7.94	3.80	4.39	5.78	6.71	8.00					
y_2 [cm]	<i>att.</i>					<i>detached no oscillation</i>					<i>attached</i>					<i>det.</i>					<i>attached</i>									
	y_1^*					y_1^*					y_1^*					y_1^*					y_1^*									
						$\tau = 30$ s					$\tau = 90$ s					$\tau = 10$ s					$\tau = 10$ s									
30																														
29																														
28																														
27																														
26																														
25																														
24																														
23																														
22																														
21																														
20																														
19																														
18																														
17																														
16																														
15																														
14																														
13																														
12																														
11																														
10																														
9																														
8																														
7																														
6																														
5																														
4																														
3																														
2																														
1																														
0																														

y_1^* = value of y_1 that marks attached and detached reflection
 y_{1p} = value of y_1 that marks periodic oscillations in the S-jump
 τ = oscillation period in S-jump
 0.77 = Froude number value in the subcritical downstream flow
 V = V-jump
 ML = Mixtilinear jump
 R = Repelled jump

S = Spatial jump
 Ba = B-jump aired
 Bna = B-jump non aired
 Ud = Undulated jump downwards curved
 Uu = Undulated jump upwards curved
 T = Transition jump
 CL = Classic jump

wave breaks and again the Bna-jump occurs at time $t = \tau$. The period τ proved to be about 15 s. This phenomenon is analogous to that described by Hager and Bretz [8] and by Ohtsu and Yasuda [20] for drop only, in the change from B-jump to Undulated jump (Fig. 1).

Comparison of the columns relative to y_1 values close to one another shows that, with an increase in F_1 , the value of y_2 that marks the passage from one jump type to the following increases. For example, the passage from R to Ba-jump for $y_1=2.71$ cm and $F_1=2$ occurs with $y_2=8$ cm; for $y_1=2.68$ cm and $F_1=6$ it occurs

with $y_2=18$ cm. Indeed, for a given flow pattern, relative to a certain jump type, with an increase in F_1 for a fixed y_1 , the velocity of the supercritical flow increases, and hence a larger depth y_2 of the subcritical flow is necessary, in order to balance the total momentum of the supercritical flow in that pattern.

It is interesting, also better to understand the results of the following experimental series with larger enlargement ratio ($L/l = 4/2$ and $4/1$), to dwell on the situations of attached or detached reflection and the formation of an S-jump. On the whole, the situations of attached reflection are much more numerous than the detached reflection ones, while the S-jump exists only for the smallest y_1 values and, however, for narrow ranges of y_2 . This is mainly due to the slight enlargement of the section ($L/l=4/3$), which generally allows the supercritical flow in the downstream channel to maintain a large value of the total momentum per unit width of the channel. Indeed, the narrow enlargement on one hand only slightly reduces, from Q/l to Q/L , the specific discharge in the downstream channel; on the other hand it allows the lateral pathlines of the enlarging supercritical flow to maintain large longitudinal velocities even after the reflection in section B-B, except for the smallest y_1 values to which the smallest V_1 values correspond. Moreover, the narrow enlargement does not facilitate formation either of cross velocity components or of flow fields which are considerably asymmetric with respect to the channel axis, as in the S-jump; on the contrary, it facilitates the formation of flow fields which are considerably symmetric, as in ML and R jumps. Therefore, the S-jump occurs only in situations in which the total momentum of the supercritical flow does not succeed in adequately opposing the total momentum of the subcritical flow along the whole width L .

5.2 Second experiment series ($L/l = 4/2$)

In the second experiment series the width l of the upstream channel is 20 cm ($L/l = 4/2$). The results are reported in Tab. 3.

Analysis of the table, qualitatively, largely confirms the results of the first series. The y_1^* values again decrease as F_1 increases. For the same F_1 , they are larger than the corresponding ones in Tab. 2: hence, the experimental situations with attached and detached reflection are partially balanced. At the same time, the presence of S-jumps considerably increases. The S-jump now always occurs after the R-jump ($y_1 > y_1^*$), though for narrow y_2 ranges. Moreover, existence ranges of S-jump after the V-jump ($y_1 < y_1^*$) considerably extends. Both circumstances are consequences of the increased relative enlargement of the section, because of which, for fixed F_1 and y_1 , the mean discharge per unit width Q/L and, consequently, the total momentum in the downstream channel proves to be decreased with respect to the first experiment series. Besides, the increased enlargement fosters formation of flow fields which are considerably asymmetric with respect to the channel axis, as in the S-jump.

Indeed, in the hypotheses that (1) there are not head losses and (2) velocity distribution in the cross-sections is uniform, Bernoulli's theorem applied between sections A-A and B-B leads to the following considerations: a) the Froude number F_B of the supercritical flow in section B-B proves to be larger than F_1 ; b)

the ratio F_B/F_1 increases as L/l increases, because of the larger decrease in y_B with respect to y_1 ; c) in spite of the increase in the ratio F_B/F_1 , the total momentum in section B-B decreases as L/l increases, because of the decrease in the specific discharge Q/L . Despite the inaccuracy of the aforesaid hypotheses, it is likely that even in the real case, for the same F_1 and y_1 , from the first to the second series the flow in section B-B will prove to be more hypercritical (i. e. F_B/F_1 will increase), while the total momentum will decrease. In the present series, in many cases the decrease in total momentum prevails over the larger hypercriticality.

Moreover about the S-jump, in this series periodic oscillation of the virtual line FG and simultaneous change in the streamlines around the spindle are observed. Indeed, these phenomena were observed only for $F_1 \geq 3$, and in particular only for y_1 values smaller than a certain $y_{1,p}$ depending on F_1 . As for the y_1^* values, the y_1 ranges within which the $y_{1,p}$ values fall are underlined by a thick line over the sequences: e.g., for $F_1=3$, $y_{1,p}$ proves to be between $y_1=1.60$ cm and $y_1=2.50$ cm. The table shows that $y_{1,p}$ decreases as F_1 increases, confirming that the S-jump is a very complex phenomenon that essentially originates from an instability situation in the equilibrium between the total momenta of the supercritical flow and the subcritical flow. The former is mainly concentrated in the middle of the downstream channel, while the latter is almost uniformly distributed on the whole section. The period τ of the oscillations observed is also reported in Tab. 3, and varies between 10 and 90 s.

Finally, by comparison of the columns in Tabs. 2 and 3 having the same F_1 , a close y_1 and the same reflection type (attached or detached), it is recognised that, increasing the enlargement ratio L/l , there is a decrease in the value y_2 that marks the change from one jump type to the next. For example, for $L/l=4/3$ (Tab. 2), $F_1=5$ and $y_1=2.63$ cm ($>y_1^*$) the R-jump occurs for $y_2=14.9$ cm; for $L/l=4/2$ (Tab. 3), $F_1=5$ and $y_1=2.66$ cm ($>y_1^*$) the R-jump occurs for $y_2=12.8$ cm. This result is an immediate consequence of the decrease in the discharge Q/L , with the same F_1 and y_1 , from the first to the second experiment series, a decrease that first affects the total momentum per unit width of the supercritical flow.

5.3 Third experiment series ($L/l = 4/1$)

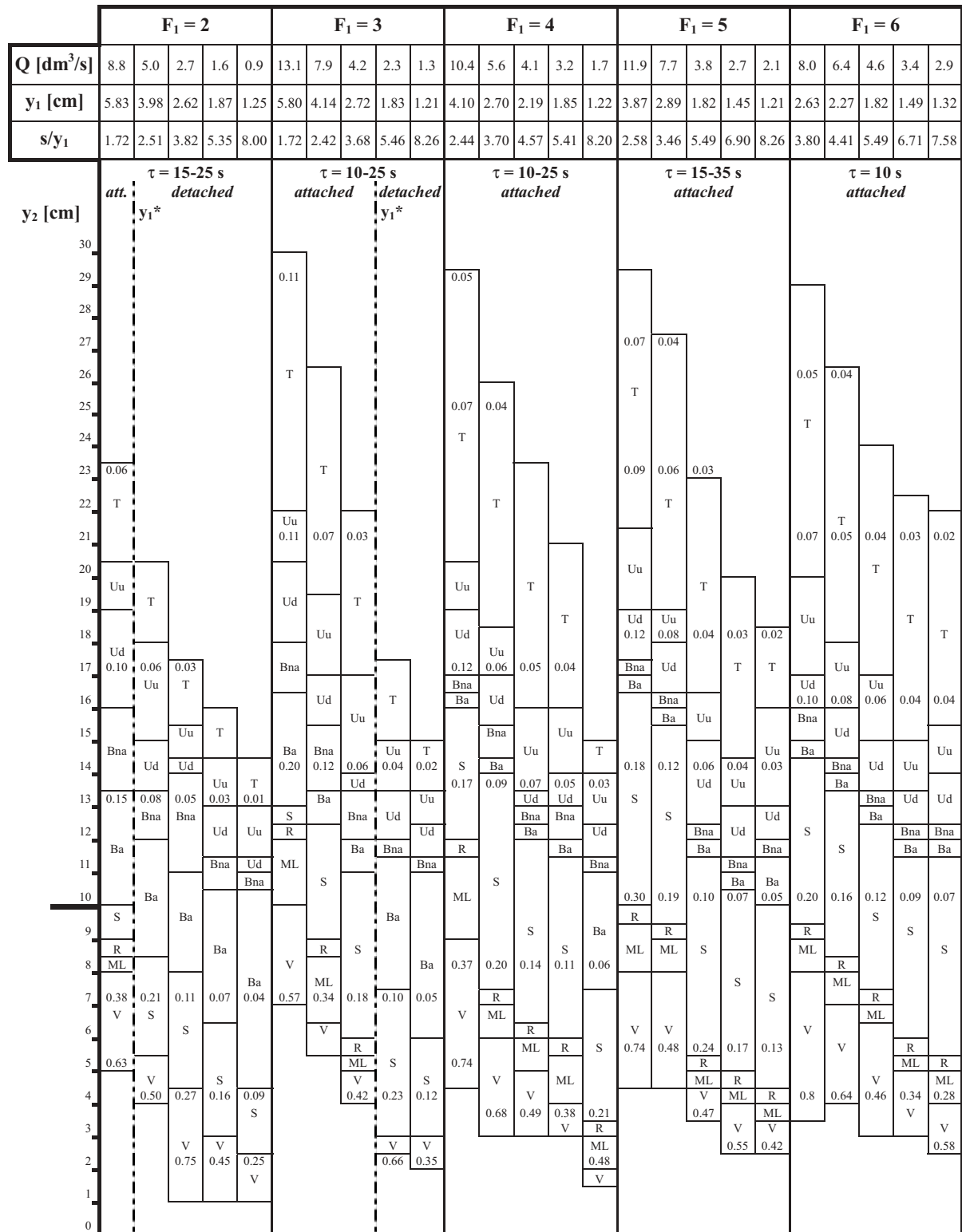
In the third experiment series the width l is 10 cm ($L/l=4/1$). The experimental results are reported in Tab. 4.

The y_1^* values generally prove to be smaller with respect to the second experiment series, and, for the larger F_1 values, also with respect to the first experiment series. Therefore, the experimental situations with $y_1 > y_1^*$ (attached reflection) become prevalent again. This result seems to demonstrate that, when L/l becomes large, in order to contrast the total momentum of the subcritical flow, the increase in the hypercriticality of the downstream flow prevails over the decrease in the total momentum of the same flow.

However, the increased enlargement causes an increase in the presence of the S-jump, which always occurs after the R-jump or after the V-jump within larger y_2 ranges, and always with the periodic phenomena, whose period τ falls between 10 and 35 s.

The y_2 values that, for the same F_1 and s/y_1 , mark the changes

Tab. 4 Sequences of jumps for $L/l = 4/1$.



y_1^* = value of y_1 that marks attached and detached reflection
 τ = oscillation period in S-jump
 0.48 = Froude number value in the subcritical downstream flow
 V = V-jump
 ML = Mixtilinear jump
 R = Repelled jump

S = Spatial jump
 Ba = B-jump aired
 Bna = B-jump non aired
 Ud = Undulated jump downwards curved
 Uu = Undulated jump upwards curved
 T = Transition jump

from one jump type to the next are further reduced. The return, in this series, to a majority of situations with attached reflection and the increased presence of S-jump is probably because, with an increase in L/l , the overall flow pattern moves

closer to that of enlargement only. Indeed, none of the authors that have studied enlargement only describes detached reflection situations, even if they carried out experiments with L/l values much larger than ours. However, they describe a jump analogous

to our S-jump.

In short, when the enlargement ratio increases, there is an increase in the presence of S-jump, a typical tridimensional flow that, in fact, is not found very much for enlargement ratios a little larger than one.

At the end of this experimental research, it is interesting to consider the fact that, leading a symmetric stream into a symmetric channel, an hydraulic phenomenon that, on the contrary, is strongly asymmetric sometimes occur. Indeed, the situations with a symmetric flow have been observed for the lower values of the depth y_2 (ML and R jumps) and for the larger ones (Ba, Bna, U and T jumps), while the situations with an asymmetric flow (S-jump) for the middle y_2 values. This observation, in the light of the physical explanations given in sections 4 and 5, suggests that the *symmetric* flow fields form when the phenomenon is altogether 'dominated' either by the upstream supercritical flow (ML and R jumps) or by the downstream subcritical flow (Ba, Bna, U and T jumps). The *asymmetric* flow field of the S-jump then appears as a transition phenomenon between two situations where the symmetry is imposed by the respective dominant stream. When the upstream flow dominates, the *enlarging* supercritical flow, downstream of the drop section, has a total momentum prevailing over that of the subcritical flow: the supercritical flow succeeds in occupying the whole width L of the channel, and the jump front locates downstream of section B-B. When the subcritical flow dominates, its total momentum is so large that it succeeds in submerging the enlarging supercritical flow, and in going upstream to the drop (sec. A-A): the phenomenon then is assimilable to a jet that flows into a water body. In the S-jump, the total momentum of the subcritical flow of course is larger than the one of the enlarging supercritical flow, in the sec. B-B, but not enough to submerge it completely. The supercritical flow, on the other hand, presents a width swiftly decreasing upstream, and depth and velocity varying in each cross section. When, at the end of R-jump, a slight increase in the depth y_2 causes the front crosses section B-B (front break), it begins to migrate upstream, searching for a new equilibrium position. Well, in the hypotheses of (1) head losses absence along the enlarging supercritical flow, (2) cross sections of the latter flow always rectangular, and (3) uniform velocity distribution in each section, application of Bernoulli's theorem along this flow allows one to recognize that the total momentum slightly decreases upstream. Thus, neglecting contribution of the two side flows, which would probably be very low, while the jump front moves upstream, it finds sections that have a decreasing total momentum, even if very slightly, and moreover this total momentum is concentrated in a more and more narrow portion of the channel width. The two circumstances explain, on one hand, that the subcritical flow succeeds in climbing up to the drop (section A-A), and, on the other hand, that it circles the enlarging supercritical flow along the side walls rather than submerging it. Remembering the slight difference between the total momenta of the two flows, it is probable that the strong turbulence, both of the enlarging supercritical flow and of the drawing back jump roller, is enough to determine an instantaneous imbalance between the flows along the two walls, that none of the two flows is then able to re-balance. In such a context, the

total phenomenon takes on the asymmetric set-ups previously described.

6 Conclusions

The hydraulic jumps that occur at an abrupt increase in the section of a rectangular channel, due to the simultaneous presence of a drop and an enlargement, are experimentally examined.

The experiments first showed that, when drop and enlargement are combined, as the depth of the downstream subcritical flow increases, several hydraulic jump types occur, which are very different from one another. Several characteristics of a certain jump type change as the 'enlargement ratio' L/l of the section, the Froude number F_1 of the upstream supercritical flow and the relative drop height s/y_1 vary.

As the depth of the downstream subcritical flow increases, two sequences of hydraulic jumps occur, depending on whether the depth y_1 is larger or smaller than the discriminant value y_1^* , which depends on L/l , F_1 , s and L .

The first sequence, for $y_1 > y_1^*$, includes the hydraulic jumps called: *V-shaped*, *Mixtilinear*, *Repelled*, *Spatial*, *B*, *Undulated* and *Transition*. The first four are mainly referable to the jumps of enlargement only, the others to those of drop only. Up to the Repelled-jump, downstream of the impact point of the nappe with the bottom, a supercritical flow is observed that enlarges until it occupies the whole width L of the downstream channel, reflects on the walls (attached reflection) and goes on downstream. The flow then becomes subcritical through a hydraulic jump whose front is clearly localised. This situation ends when the front of the Repelled-jump breaks. Then, along a wall, the subcritical flow moves upstream up to the drop, while the supercritical flow is deflected toward the opposite wall (*Spatial-jump*): now a clearly localised jump front is not distinguished.

In the second sequence, for $y_1 < y_1^*$, the front break already occurs in the *V-jump*, after which the *Spatial-jump* forms, followed – as in the first sequence – by the *B*, *Undulated* and *Transition* ones. Then, the enlarging supercritical flow in the downstream channel does not reflect on the walls (detached reflection). For the two behaviours a common physical explanation has been recognised in the fact that, for given L , L/l , F_1 and s , the smaller depth y_1 is the smaller the velocities and total momentum of the downstream supercritical flow are.

Comparison between the three experiment series points out that, as L/l increases, the presence of *Spatial-jump*, characteristic of enlargement, increases, because of the marked tridimensionality of the flow. For L/l slightly larger than one, *Spatial-jump* forms only for the smallest y_1 values, probably for the same reasons as given for attached or detached reflection.

In *Spatial-jump*, several periodic phenomena are observed, analogous to those reported by other authors for enlargement only. These phenomena, absent for L/l slightly larger than one, are obviously more marked for larger values. In the formation of *Undular-jump* other periodic phenomena are observed, reported by other authors for drop only. The latter, by contrast, only exist for L/l slightly larger than one.

In conclusion, hydraulic jumps at a drop combined with an abrupt

enlargement present very different and complex characteristics. In this paper these characteristics are recognised and described, and explanations, which are mainly qualitative, are given for them. The latter constitute an indispensable framework for the observed phenomena, governed by the parameters mentioned above. Determination of the quantities necessary to design the device obviously requires specific experimental investigations for each type of hydraulic jump that can occur with variations in the aforesaid parameters.

Acknowledgements

The authors thank Dr Luigi Gangitano, who carefully carried out the experiments for the present paper.

The research was carried out with the financial support of the Italian Ministry for the University and for Scientific and Technologic Research (M.U.R.S.T. 60%).

References / Bibliography

- BREMEN R. and HAGER W.H., 1990, Ressautes hydrauliques dans les canaux avec elargissement. *Proc. of XXII Convegno di Idraulica e Costruzioni Idrauliche*, Cosenza, Italy, Vol. 1, pp. 171-182.
- CHOW V.T., 1959, *Open channel hydraulics*, McGraw-Hill.
- FERRERI G.B. and FERRO V., 1990, Sideways-free overfall of a subcritical flow in rectangular channels (in italian; original title: 'Efflusso non guidato di una corrente lenta da un salto di fondo in canali a sezione rettangolare'). *Proc. of XXII Convegno di Idraulica e Costruzioni Idrauliche*, Cosenza, Italy, Vol. 1, pp. 195-213.
- FRENCH R.H., 1986, *Open channel hydraulics*, McGraw-Hill.
- GANGITANO L., 1992, *Hydraulic jump phenomena at abrupt changes of section* (in italian; original title: 'Fenomeni di risalto idraulico in corrispondenza di brusche variazioni di sezione'), graduation thesis, Dept. of Hydraulic Engineering and Environmental Applications, University of Palermo (Italy).
- HAGER W.H., 1985, Hydraulic jump in non-prismatic rectangular channels, *Journal of Hydraulic Research*, Vol. 23, No. 1, pp. 21-35.
- HAGER W.H., 1985, B-jumps at abrupt channel drops, *Proc. ASCE, Journal of Hydraulic Engineering*, Vol. 111, No. 5, pp. 861-866.
- HAGER W.H. and BRETZ V.N., 1986, Hydraulic jumps at positive and negative steps, *Journal of Hydraulic Research*, Vol. 24, No. 4, pp. 237-253.
- HAGER W.H. and BRETZ V.N., 1987, Reply on 'Hydraulic jumps at positive and negative steps' by themselves, *Journal of Hydraulic Research*, Vol. 25, No. 3, pp. 411-413.
- HENDERSON F.M., 1966, *Open channel hydraulics*, Macmillan.
- HERBRAND K., 1973, The spatial hydraulic jump, *Journal of Hydraulic Research*, Vol. 11, No. 3, pp. 205-218.
- KAVAGOSHI N. and HAGER W.H., 1990, Wave type flow at abrupt drops, *Journal of Hydraulic Research*, Vol. 28, No. 2, pp. 235-252.
- MOORE W.L. and MORGAN C.W., 1957, The hydraulic jump at

an abrupt drop, *Proc. ASCE, Journal of the Hydraulics Division*, Vol. 83, No. HY6, paper 1449, pp. 1-21.

MOORE W.L. and MORGAN C.W., 1959, Closure on 'The hydraulic jump at an abrupt drop' by themselves, *Proc. ASCE, Journal of the Hydraulics Division*, Vol. 85, No. HY2, pp. 87-91.

NASELLO C., 1992, Experimental research on a level stilling basin without end step (in italian; original title: 'Esame sperimentale di un dissipatore a fondo piano e senza gradino terminale per correnti a superficie libera'). *Proc. of XXIII Convegno di Idraulica e Costruzioni Idrauliche*, Florence, Italy, Vol. 4, pp. E.207-E.220.

NASELLO C., 1995, Experimental research on a level-bottom module flume (in italian; original title: 'Esperienze su un modulatore a fondo piano per canali'). *L'Energia Elettrica*, Vol. 72, n. 4, pp. 53-68.

NOSEDA G., 1963, Hydraulic jumps in enlarging supercritical flow (in italian; original title: 'La formazione del risalto lungo una corrente veloce in espansione'). *Proc. of the VIII Convegno di Idraulica*, Pisa, Italy, pp. 1-11.

NOSEDA G., 1964, An instability phenomenon of hydraulic jump in enlarging supercritical flow (in italian; original title: 'Un fenomeno di instabilità del risalto lungo una corrente veloce in espansione'). *L'Energia Elettrica*, Vol. 41, No. 4, pp. 249-254.

OHTSU I. and YASUDA Y., 1987, Discussion on 'Hydraulic jump at positive and negative steps' by Hager W.H. and Bretz V.N., *Journal of Hydraulic Research*, Vol. 25, No. 3, pp. 407-413.

OHTSU I. and YASUDA Y., 1991, Transition from supercritical to subcritical flow at an abrupt drop, *Journal of Hydraulic Research*, Vol. 29, No. 3, pp. 309-328.

RAJARATNAM N., ORTIZ V., 1977, Hydraulic jumps and waves at abrupt drops, *Proc. ASCE, Journal of the Hydraulics Division*, Vol. 103, No. HY4, pp. 381-394

RAJARATNAM N. and SUBRAMANYA K., 1968, Hydraulic jumps below abrupt symmetrical expansions, *Proc. ASCE, Journal of the Hydraulics Division*, Vol. 94, No. HY2, paper 5860, pp. 481-503.

SHARP J.J., 1974, Observations on hydraulic jumps at rounded steps, *Proc. ASCE, Journal of the Hydraulics Division*, Vol. 100, No. HY6, paper 10592, pp.787-795.

WHITE M.P., 1943, Discussion on 'Energy loss at the base of a free overfall' by Moore W.L., *Trans. ASCE*, Vol. 108, pp. 1361-64.

Notations

- F_1 Froude number of the supercritical flow in the upstream channel
- F_2 Froude number of the subcritical flow in the downstream channel
- F_B Froude number of the enlarging supercritical flow in section B-B
- g gravitational acceleration
- h_d mean piezometric head along the axis of drop wall
- k_1 critical depth of the flow in the upstream channel
- l width of the upstream channel

L	width of the downstream channel	$y_{1,p}$	y_1 value under which periodic planimetric oscillations of the virtual line 'FG' may occur in the S-jump
Q	discharge	y_2	depth of the subcritical flow in the downstream channel
Q_I, Q_{II}	discharges of the flows heading, respectively, downstream and upstream, after the incidence of the nappe with the downstream channel bottom	y_a	depth of the pool at the drop toe
s	drop height	y_B	depth of the enlarging supercritical flow in section B-B
V_1	mean velocity of the flow in the upstream channel	τ	period of the planimetric oscillation of the virtual line 'FG' in S-jump or of the longitudinal oscillation of the nappe in the change from the Bna to the Ud-jump
y_1	depth of the flow in the upstream channel		
y_1^*	y_1 value that marks the change from attached to detached reflection		